JPP Journal of Pharmacy and Pharmacology

JPP 2007, 59: 29–39

Received June 5, 2006
Accepted September 14, 2006
DOI 10.1211/jpp.59.1.0005
ISSN 0022-3573

Modification of the crystal habit of celecoxib for improved processability

Sheere Banga, Garima Chawla, Deepak Varandani, B.R. Mehta and Arvind K. Bansal

Abstract

Crystallization is often used in the pharmaceutical industry for purification and isolation of drugs, and also as a means of generating polymorphs or isomorphs. The aim of this study was to investigate the role of extrinsic crystallization parameters on the crystallized product, with special emphasis on improving the mechanical properties of acicular celecoxib. Celecoxib isomorphs were prepared using different techniques (solvent crystallization and vapour diffusion) and crystallization conditions (solvents, stirring, degree of supersaturation, crystallization temperature and seeding). Powder X-ray diffractometry, spectroscopic and thermal methods were used to investigate physical characteristics of crystals. Growth kinetics and aggregation dynamics of crystallization in polar and non-polar solvents were simulated using a dynamic light scattering method. The quick appearance of broad peaks over the range of 10–8000 nm in chloroform during crystallization simulation studies indicated faster aggregation in non-polar solvents. Aspect ratio, flow, compressibility and surface area of recrystallized products were also determined. Surface topography was determined by atomic force microscopy and the lath-shaped crystals (aspect ratio of 2–4) exhibited a roughness index of 1.79 in comparison with 2.92 for needles. Overall, the lath-shaped isomorphs exhibited improved flow and better compressibility.

Department of Pharmaceutical Technology (Formulations), National Institute of Pharmaceutical Education and Research (NIPER), Sector-67, S.A.S. Nagar, Punjab - 160 062, India

Sheere Banga, Garima Chawla, Arvind K. Bansal

Department of Physics, Indian Institute of Technology (IIT), Hauz Khaz, New Delhi-110016, India

Deepak Varandani, B.R. Mehta

Correspondence: Arvind K. Bansal, Department of Pharmaceutical Technology (Formulations), National Institute of Pharmaceutical Education and Research (NIPER), Sector-67, S.A.S. Nagar, Punjab - 160 062, India. E-mail: akbansal@niper.ac.in

Acknowledgments and funding: Mr Martin Martinez-Ripoll (Departamento de Cristalografica, Instituto de Quimica-Fisica Rocasolano, Spain) and Ms Manjari Sunitha (Bioinformatics Centre, University of Pune, India) are gratefully acknowledged for providing the single crystal X-ray diffraction data of celecoxib. Garima Chawla is grateful for financial assistance provided by CSIR, India.

Introduction

A solid substance is characterized by its internal structure and external appearance (habit), both of which critically impact the physicochemical and mechanical properties and, thus, the manufacturing of solid dosage forms. Apart from polymorphs, differences only in the external structure profoundly affect surface-dependent properties such as drying, dissolution, sedimentation, dispersibility, flowability, mixing pattern, compressibility, bulk density and packing behaviour (Rasenack & Muller 2002a). Isomorphism, defined as the solid-state form of a compound, with differences only in habit and no differences in internal crystal lattice, plays a critical role in solid dosage forms, especially of high-dose drugs. The processing of high-dose drugs is primarily governed by the properties of the drug, and excipients play very little role (Rasenack & Muller 2002b). Crystal habit can be quantitatively expressed in terms of aspect ratio (AR), defined as the ratio of the length (longest dimension from edge to edge of a particle oriented parallel to the ocular scale) to the width (the longest dimension of the particle measured at right angles of the length) (Brittain 2001), and values of AR approaching 1 (spherical or cubic shape) are considered to be pharmaceutically good (Lloyd 1998). It is preferable to keep the AR values below 5 so as to avoid problems with flow (Lloyd 1998).

There are numerous reports on the generation, characterization and performance characteristics of polymorphs in the literature. However, there is little information on the influence of crystallization kinetics (comprising nucleation and crystal growth) on the generation of isomorphs. Nucleation followed by crystal growth is governed by the relative rate of molecule deposition on various faces, which in turn is influenced by the strength of binding molecules at the crystal surface and the internal architecture of the crystal. Extraneous factors such as solvents, temperature, degree of supersaturation, stirring and impurities, by altering the rate of deposition on the surface, may modify not only the polymorphic form but also

the crystal habit (Berkovitch-Yellin 1985; Hornedo & Murphy 1999; Shekunov & York 2000). The critical role of crystallization kinetics in determining the crystalline form is also recognized by the US Food and Drug Administration and is described in the guidelines for the manufacture of drug substances (FDA 1987; Hornedo & Murphy 1999). The present study aimed to study the effect of crystallization conditions on crystal forms of celecoxib (CEL), a selective cyclooxygenase 2 inhibitor. CEL exhibits manufacturing and handling problems owing to its cohesive needle-shaped crystals (see Figure 1a), having high surface energy and electric charge. It has low bulk density and the needles tend to agglomerate together during mixing, which may lead to content non-uniformity during capsule filling operations. Its low compressibility does not allow the development of tablet solid dosage forms, as it forms a monolithic mass upon compression (Ferro & Miyake 2001). It is reported that CEL forms metastable polymorphs with negligible difference in melting point that are easily revertible to stable form (Ferro & Miyake 2004). Therefore, it is anticipated that modification of the crystal habit will not be accompanied by polymorphic transformation. Hence, CEL is a model candidate for exploiting the crystallization process for optimizing powder properties, aimed at improving its processability.

Solvent recrystallization and vapour diffusion were used to facilitate isomorph generation of CEL with improved mechanical properties. Solvent recrystallization is the most common and convenient method for the generation of alternate solid state forms (Guillory 1999). Vapour diffusion has not been explored extensively for pharmaceuticals, but has been used previously for protein crystallization (Cang & Bi 1998). It lends an ideal ratio of nucleation rate to crystal growth, thus providing crystal growth kinetics favourable for habit modification (Grant 1999). The temporal profile of the molecular aggregation phenomenon was captured using dynamic light scattering in order to understand the crystallization kinetics. Various generated crystal forms were studied for their flow properties and compression behaviour.

Materials and Methods

Materials

CEL was a gift from Zydus Cadila Healthcare Limited, Maharashtra, India. All solvents used were either high-performance liquid chromatography grade or analytical grade.

Solubility studies

Solvents having a dielectric constant of between 1.88 and 46.70 (see Table 1) were selected based on their polarity. The saturation solubility of CEL in different solvents was determined by placing an excess amount of the drug with 1 mL of solvent in 5-mL screw capped glass vials. The vials (n = 3) were shaken in a water bath (Julabo Labortechnik GmbH, Seelbach, Germany) maintained at 70°C for 1 h. Vials were then equilibrated at 5, 25, 40 and 60°C without stirring to determine the saturation solubility at these temperatures. Samples were withdrawn after 6 h, filtered using 0.22-μm nylon filters and analysed after appropriate dilution using a UV spectrophotometer (Lambda 20; Perkin-Elmer Corp., CT, USA) at 252 nm.

Crystallization experiments

Solvent crystallization

A protocol for solvent recrystallization was developed for each solvent using different degrees of supersaturation (x + 25%, x and x – 25%, where x is the saturation solubility), temperatures (5, 25, 40, 60°C), presence and absence of stirring, and variation in the duration of stirring (– ½T_s and T_s, where T_s is the time to crystallization). Accurately weighed amounts of CEL (as determined by solubility studies) were dissolved in 1 mL of solvent to obtain defined drug concentrations. The solution was then filtered into jacketed glass vessels and allowed to evaporate at the desired temperatures. Temperature was maintained during the crystallization experiments by water recirculation in jacketed vessels (Heto, Allerod, Denmark), and stirring at 800 rev min^{-1} was achieved using magnetic stirrers (Eutech, Instruments, Vernon Hills, IL, USA). The crystals were then collected, dried at room temperature and used for further characterization.

Vapour diffusion technique

Hexane, cyclohexane and carbon tetrachloride were selected as "antisolvents", while chloroform, ethyl acetate, tetrahydofuran, isopropanol, acetone, ethanol, methanol and acetonitrile were selected as "solvents". This was based on the miscibility of antisolvents with solvents and similarity in their boiling range (see Table 2). Accurately weighed amounts of CEL (as determined by solubility studies) were dissolved in 1 mL of solvent to provide saturated solution at room temperature. The solution was then filtered into a 5-mL glass beaker and transferred to a 50-mL tightly closed screw-cap bottle containing 15 mL antisolvent. The crystals were collected after complete evaporation of the solvent and dried at room temperature. Crystallization in the absence of antisolvents at the same temperature conditions served as a control.

Characterization of crystallized products

Microscopy

The crystal habit was observed at different magnifications both with and without silicon oil under optical and polarized light using a Leica DMLP polarized light microscope (Leica, Wetzlar, Germany) equipped with IM 50 V1.20 Twain module imaging software (Leica). The birefringence pattern was viewed under cross polarizers. Particle size was determined using a pre-calibrated stage micrometer by taking longest dimension of the crystal for a minimum of 100 particles and from that AR was calculated.

Powder X-ray diffraction (PXRD)

PXRD patterns of samples were recorded at room temperature on an X-ray powder diffractometer (D8 Advance; Bruker, Madison, WI, USA) using CuKα radiation (= 1.54 Å) at 35 kV, 30 mA, passing through a nickel filter. Data was collected in a continuous scan mode with a step size of 0.01°

and step time of 1 s over an angular range of 3° to 40° 2θ. The diffraction data were obtained as the sample holder was rotated. The sample holder was rotated so as to reduce the orientation effect. Recorded diffractograms were analysed with EVA diffraction software (Bruker).

Thermal characterization

Differential scanning calorimetry (DSC), thermogravimetric analysis (TGA) and hot-stage microscopy (HSM), and spectroscopic characterization using Fourier transform infrared spectroscopy (FTIR) were done as reported previously (Chawla et al 2003).

Atomic force microscopy (AFM)

AFM was carried out using a Nanoscope III A (Digital Instruments, Veeco Metrology Group, Santa Barbara, CA, USA) operated at room temperature in the tapping mode. The samples to be imaged were pasted on a clean silicon substrate fixed on to the standard sample holder using double-sided adhesive tape. Silicon tips (RTESP) vibrating at their resonant frequency were used to obtain the height images at a slow scanning speed of 0.5 Hz.

Surface area measurement

Surface area was determined using nitrogen gas sorption (SMART SORB 91 Surface Area Analyzer; Micrometrics, Norcross, GA, USA). Before measurements, weighed samples were regenerated by degassing to remove moisture and contamination (Flow Prep 060; Micrometrics). The regenerated sample was dipped in liquid nitrogen and the quantity of the adsorbed gas was measured using a thermal conductivity detector and then integrated using an electronic circuit in terms of counts. The instrument was calibrated by injecting a known quantity of nitrogen. The measured parameters were then used to calculate the surface area of the sample by employing the adsorption theories of Brunauer, Emmett and Teller (Martin et al 1997).

Crystallization kinetics using dynamic light scattering

The events of crystallization were observed in both polar (methanol) and non-polar solvent (chloroform), and were studied using a dynamic light scattering approach in a Zetasizer Nano ZS (Malvern instruments, Malvern, UK). Sample preparation involved dissolving accurately weighed CEL in methanol and chloroform, to yield an undersaturated (x – 25%) solution at a temperature of 25°C. The solution was then filtered through a 0.22-μm filter into the glass cuvette of the Zetasizer. Sample preparation was carried out in a laminar flow bench (Sonar; Associated Scientific Technologies, New Delhi, India). Measurements were made until the size limit of the Zetasizer (10 μm) with the help of software at 10-min intervals in terms of correlation coefficient, average size, width of the peaks, intensity statistics, volume particle size distribution, volume statistics, number particle size distribution, number statistics and other size diagnostics.

Measurement of flow properties

Samples were sieved through a BSS #18 sieve with and without the addition of Aerosil 200 (2% w/w), and bulk and tap density were calculated using the USP tapping method. Carr's index and Hausner ratio were calculated as markers for flowability.

Compression studies

After sieving through a BSS #18 screen, laths and acicular crystals were studied for their compression behaviour. All experiments were done with a 50-kg load cell using a 10-mm flat-faced die punch set on a texture analyser (TA-XT 2i; Stable Microsystems, Surrey, UK), at a sample weight of 260 ± 5 mg (n = 10). Two methods were used: one where the force required to travel a particular distance (4 mm) was measured; and one where the distance travelled by the punch to attain a force of 450 N was determined.

The initial position of the upper punch was kept constant in all the experiments using the calibration scale. The other parameters, punch travel speed of 1 mm s^{-1} before and after the test, 0.1 mm s^{-1} during the test and a trigger/stimulus of 0.05 N were set to activate after travelling a distance of 1 mm. Net work done was calculated from the area under the curve.

Statistical analysis

Statistical analysis was performed to assess the effect of solvents on crystal habit during vapour diffusion. Width of the crystals was used as the quantitative parameter for comparison of laths, thin laths and needles in Kruskal–Wallis one-way analysis of variance by ranks (SigmaStat version 2.03; Systat Software Inc., San Jose, CA, USA). In the case of flow measurements, the *t*-test was applied to individual groups: needles and laths; needles and laths with 2% Aerosil 200; needles and laths passed through BSS #18 sieves; and needles and laths passed through BSS #18 sieves with 2% Aerosil 200. A level of $P < 0.01$ denoted significance in all cases.

Results and Discussion

Solubility studies

The solubility of the solute should be over the range of 5–200 mg mL^{-1} at room temperature for a solvent to be used for recrystallization purposes (Gua et al 2004). Table 1 gives the saturation solubility of CEL in different solvents at different temperatures along with the boiling points and dielectric constants of the solvents. An increase in solubility with rise in temperature from 5 to 60°C was observed in all solvents. CEL was found to be practically insoluble in low polarity solvents such as hexane (0.08 mg mL^{-1}) and cyclohexane (0.08 mg mL^{-1}) even at 60°C. In contrast, in polar solvents, an increase in solubility was observed with increase in dielectric constant, indicating favourable solute–solvent interactions. Apart from solubility, solvent selection also depends on physical properties such as boiling point, viscosity, surface tension and toxicity issues as specified in ICH guidelines (ICH Harmonized Tripartite Guidelines 1997). Among the various solvents listed in Table 1, not all solvents were suitable for crystallization due to limitations such as high melting point, poor solubility of CEL, low evaporation rate, high viscosity, and ability of CEL to form solvates (Chawla et al 2003). The

Table 1 Solubility of celecoxib in different solvents at different temperatures

Solvent (bp°C)	Dielectric constant	Saturation solubility at different temperatures (mg mL^{-1})			
		5°C	25°C	40°C	60°C
Hexane (68.7)	1.88	0.03 (0.001)	0.06 (0.005)	0.07 (0.003)	0.08 (0.004)
Cyclohexane (80.7)	2.00	0.03 (0.002)	0.06 (0.001)	0.07 (0.003)	0.08 (0.001)
Carbon tetrachloride (76.8)	2.20	6.31 (0.35)	8.16 (0.87)	8.74 (0.55)	10.98 (0.54)
Toluene (110.6)	2.38	10.26 (0.95)	11.10 (0.78)	13.97 (0.67)	15.36 (0.83)
Chloroform (61.2)	4.80	8.61 (0.43)	11.11 (1.02)	16.76 (0.78)	21.84 (0.46)
Ethyl acetate (77.1)	6.02	121.91 (2.01)	136.86 (1.32)	167.60 (2.34)	180.47 (0.98)
Tetrahydrofuran (66.0)	7.58	707.37 (5.61)	831.98 (2.10)	872.27 (2.76)	922.11 (3.86)
Dichloromethane (39.8)	8.90	25.46 (0.42)	31.23 (0.32)	–	–
Benzyl alcohol (205.3)	13.10	85.77 (1.21)	92.00 (0.96)	121.04 (2.13)	127.10 (3.10)
Methyl isobutyl ketone (116.5)	13.10	146.41(1.44)	165.10 (2.00)	183.38 (0.87)	209.34 (2.89)
Butanol (117.7)	17.50	11.83 (0.34)	13.31 (0.65)	27.93 (1.50)	31.93 (2.75)
Isopropyl alcohol (82.3)	19.90	10.96 (1.43)	11.09 (2.01)	14.84 (0.98)	15.34 (1.35)
Acetone (56.3)	20.70	630.25 (3.60)	650.00 (2.68)	684.00 (4.24)	689.00 (1.74)
Ethanol (78.3)	24.55	50.51 (1.23)	57.94 (2.50)	83.88 (1.69)	88.36 (2.44)
Methanol (64.7)	32.60	162.61 (1.62)	179.64 (1.88)	221.18 (2.04)	235.72 (3.78)
Acetonitrile (81.6)	37.50	244.23 (3.45)	257.94 (2.22)	293.87 (3.54)	314.22 (4.04)
Dimethyl sulfoxide (189.0)	46.70	794.18 (4.12)	826.16 (3.68)	836.96 (2.11)	847.35 (4.45)

Values are mean (s.d.), n = 3.

following solvents were used for further crystallization experiments: carbon tetrachloride, toluene, chloroform, ethyl acetate, dichloromethane, tetrahydrofuran, methyl isobutyl ketone, butanol, isopropyl alcohol, acetonitrile, acetone, ethanol and methanol. The crystallization experiment with dichloromethane was conducted only at the lower temperatures of 5 and 25°C because of its lower boiling point. In the case of vapour diffusion, based on solubility studies and miscibility, solvents were classified into antisolvents and solvents. A solvent in which the drug has solubility over the range of 5–200 mg mL^{-1} is referred to as solvent, in contrast to the antisolvent in which the drug has poor solubility, preferably <1 mg mL^{-1} (Guillory 1999).

Crystallization using solvent crystallization and vapour diffusion

The protocol developed for solvent recrystallization involved the use of different solvents, temperatures and stirring, as they were expected to allow variable solute–solvent interaction, evaporation rates and mass transfer kinetics, respectively (Akal et al 1986; Hulliger 1994).

Effect of crystallization parameters

Effect of crystallizing solvent

Solvents have been reported to affect the crystal habit by preferential adsorption of solvent molecules on specific faces, thus delaying their growth rate (Berkovitch-Yellin 1985). However, there are no consistent prediction methods for the effect of solvent on crystal morphology. Solvent polarity controls solvent–solute interactions that affect the crystallization kinetics and consequently the appearance of isomorphs. In addition to the solvent–solute interaction at the molecular level, bulk properties of solvents, such as viscosity and surface tension may also affect the appearance of isomorphs (Gua et al 2004). On shifting towards non-polar solvents, a modification in crystal habit was observed (Figure 1). The AR in polar solvents was as high as 9.4 in comparison with 5–6 in non-polar solvents, and in the case of carbon tetrachloride, toluene and chloroform at 60°C and x – 25% concentration, the AR values were as low as 2.8, 2.8 and 3.2, respectively. High solubility of CEL in polar solvents (methanol, butanol, methyl isobutyl ketone, acetone, acetonitrile and isopropyl alcohol) promotes rapid nucleation and probably led to development of acicular crystals. Also, as reported previously with phenytoin, decreased interfacial tension in polar solvents leads to favourable solute–solvent interactions causing a transition from a smooth to a rough interface at all faces, thus resulting in rapid crystallization (Lahva & Leiserowitz 2001; Nokhodchi et al 2003). On the other hand, poor solubility of CEL in non-polar solvents (chloroform, toluene and carbon tetrachloride) gave lower solute content, leading to predominance of crystal growth phenomenon over nucleation.

Events attributed to Brownian motion of molecules and aggregates over the size range of 1 nm to 1 μm occurring during crystallization in polar and non-polar solvents were captured by dynamic light scattering in the Zetasizer. However, in a dynamic crystallizing system, solution concentration is expected to increase with time, leading to multiple scattering and lower signal-to-noise ratio. Use of backscattering provided by NIBS (non-invasive back scattering) helped to overcome this problem and allowed the use of higher concentrations, (max. up to 50–60% w/v). Undersaturated (x – 25%) solutions in methanol (representative polar solvent) and chloroform (representative non-polar solvent) with 134.73 mg mL^{-1} and 8.33 mg mL^{-1} of CEL, respectively, were found to be well within the detection limits of the Zetasizer (10–600 mg mL^{-1}).

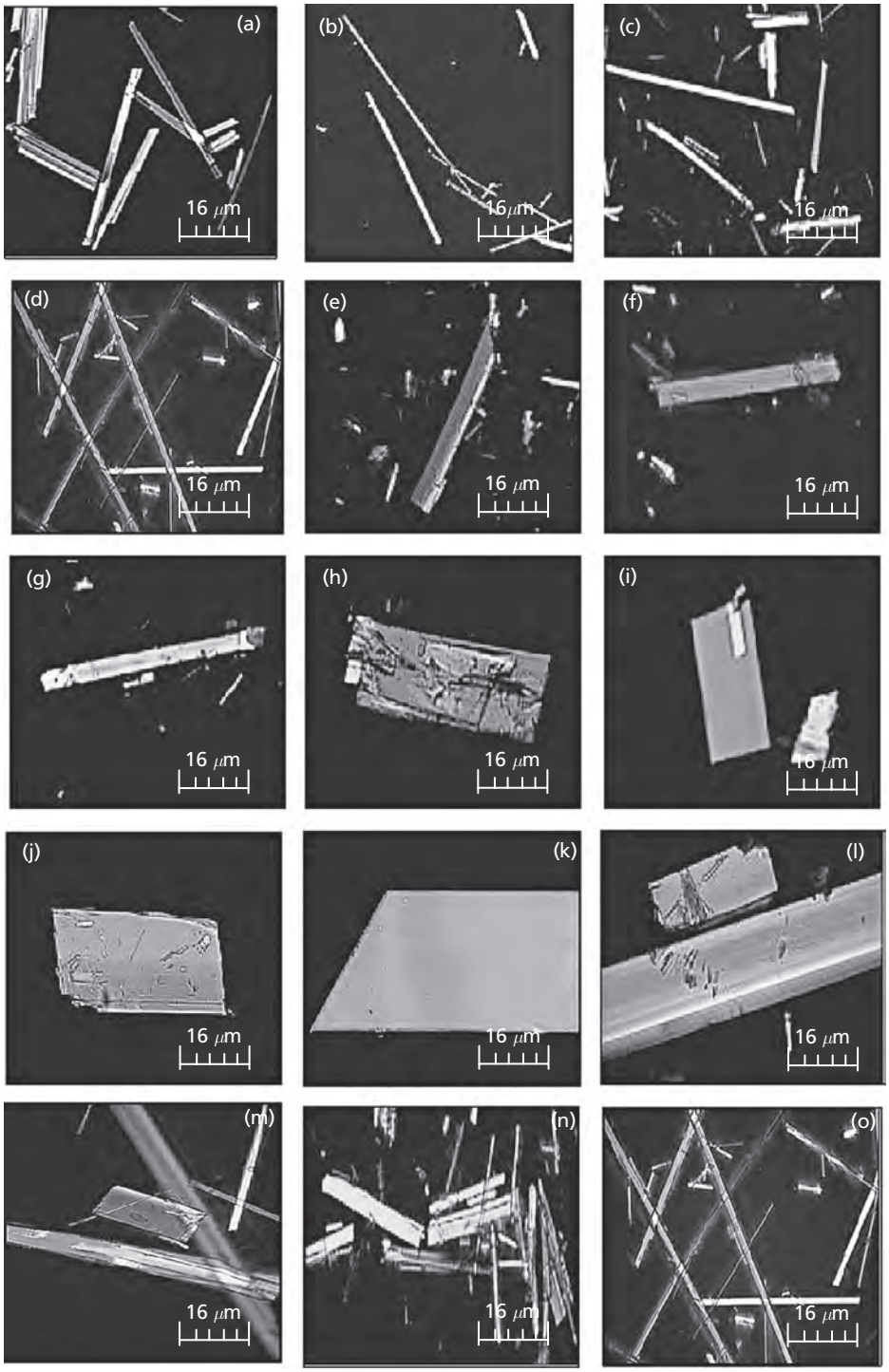

Figure 1 Polarized photomicrographs of solvent crystallized and vapour diffusion products at 63× (×10): (a) pure drug; (b) recrystallized from ethanol, T = 25°C, concentration = x; (c) recrystallized from methanol, T = 25°C, concentration = x; (d) recrystallized from butanol, T = 25°C, concentration = x; (e) recrystallized from toluene, T = 25°C, concentration = x; (f) recrystallized from chloroform, T = 25°C, concentration = x; (g) recrystallized from carbon tetrachloride, T = 25°C, concentration = x; (h) recrystallized from toluene, T = 60°C, concentration = x – 25%; (i) recrystallized from chloroform, T = 60°C, concentration = x – 25%; (j) recrystallized from carbon tetrachloride, T = 60°C, concentration = x – 25%; (k) vapour diffusion product using chloroform as solvent and hexane as antisolvent at T = 25°C; (l) vapour diffusion product using ethyl acetate as solvent and hexane as antisolvent at T = 25°C; (m) vapour diffusion product using tetrahydrofuran as solvent and hexane as antisolvent at T = 25°C; (n) vapour diffusion product using isopropanol as solvent and hexane as antisolvent at T = 25°C; (o) vapour diffusion product using methanol as solvent and hexane as antisolvent at T = 25°C.

Crystallization is a dynamic process in which aggregation and deaggregation proceed simultaneously until nuclei are formed; the results were interpreted based on correlograms and intensity distribution and not on the basis of average particle size. The samples undergoing crystallization exhibited a broad distribution of size, with polydispersity index greater than 0.5 in most of the readings. In the case of the Zetasizer, the particle size measured is the diameter of the sphere that diffuses at the same speed as the particle being measured and the size is determined by first measuring the Brownian motion of the particles in a sample using dynamic light scattering. The fluctuations in scattering intensity are measured and used to calculate the size of particles within the sample, after which the digital correlator measures the degree of similarity between two signals over a period of time. In the correlogram, the results are measured in terms of correlation coefficient with time (from 500 ns to 3 s) and the angle θ represents the polydispersity of distribution. In the case of small particles, the correlation is lost sooner and the decay is faster compared with larger particles, which show correlation for longer. In both the solvents, a sharp initial fall in the correlation coefficient was observed for up to 2 h, indicating that the system is mostly composed of small particles. Also, a lower θ value, indicative of the type of distribution, suggested that initially there was a narrow size distribution. In both the solvents beyond 10 h, decay in the correlation coefficient was observed with larger θ values, representing the presence of aggregates and broader size distribution in the system (Figure 2a, b). Thus, with time, a shift was observed from individual molecules to aggregates having higher polydispersity.

Differences were observed in the intensity distribution pattern (% intensity vs size) of methanol and chloroform. In methanol, a single peak at 0.7–1.2 nm was observed for the initial 2 h and later a broad peak over the range of 1000 to 5500 nm developed, and after 10 h only the latter peaks remained. On the other hand, in chloroform, the aggregation rate was quite fast and the initial peak at 0.7–1.2 nm subsided after 5 min. Other broad peaks started to appear over the range of 10–50, 100–800 and 3000–8000 nm within 5 min (Figure 3a, b), and after 10 h only the latter peaks remained. This suggested that faster aggregation dynamics existed in non-polar solvents compared with polar solvents and solute–solvent interactions were less favoured in chloroform. There are no previous reports on the use of the Zetasizer for the characterization of small molecules. Zetasizer has been previously used to study the kinetics of protein crystallization and in the determination of conditions for crystallization. Studies have been conducted to quantify and detect aggregation, sample polydispersity, melting point and thermal denaturation of proteins (detailed specification sheets available from: www.malvern.co.uk/zetasizernano). In the case of pharmaceuticals, an attempt has been made to assess the comparative contribution of nucleation and crystal growth towards the overall crystallization phenomenon. This would also help clarify the underlying mechanism of solvent-induced habit change without occurrence of polymorphism/pseudopolymorphism, allowing the experimental parameters to be further optimized. The method offers a number of advantages: it is rapid, requires low sample volumes, has high sensitivity, requires no complex sample manipulations and delivers rapid and extensive information. Moreover, the studies can be extended to see the effect of temperature on crystallization.

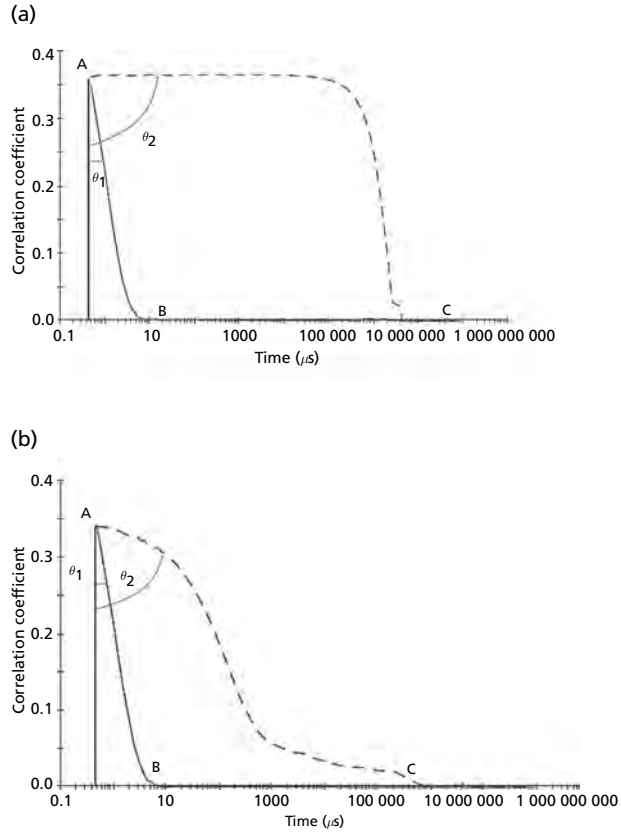

Figure 2 Correlograms obtained from Zetasizer captured during a crystallization event in a 12-mm quartz glass, square cuvette using polar and non-polar solvents. (a) Methanol (temperature 25°C, count rate 328 kcps, measurement position 0.85 nm, material refractive index 1.333, dispersant refractive index 1.326, viscosity o.59 cP, attenuator 6). (b) Chloroform (temperature 25°C, count rate 178 kcps, measurement position 4.65 nm, material refractive index 1.333, dispersant refractive index 1.442, viscosity 0.54 cP, attenuator 11). Curve AB represents the initial reading after 5 min and curve AC is the reading after 10 h in both solvents. Results are a sum of accepted data collected.

Degree of supersaturation

The solute content in the crystallizing solution together with the temperature were found to critically impact the final product. Whereas acicular crystals were observed under high supersaturation conditions (x + 25%) in all solvents at all crystallizing temperatures, large broad crystals (AR values of 2–4) were obtained under low supersaturation conditions (x – 25%) in non-polar solvents at 60°C. The results are in agreement with earlier studies, in which acicular crystals were formed under higher supersaturation conditions (Tiwary 2001). High supersaturation has been reported to provide an initial surge for molecular aggregation, rapid induction of nucleation and quick decay of supersaturation, resulting in faster crystallization (Hornedo & Murphy 1999). Lower temperatures also lead to higher supersaturation and increased nucleation. Once the nuclei are formed crystal growth promotes further development of crystals (Takubo & Kume 1984; Granberg et al 1999). On the contrary, lower concentrations

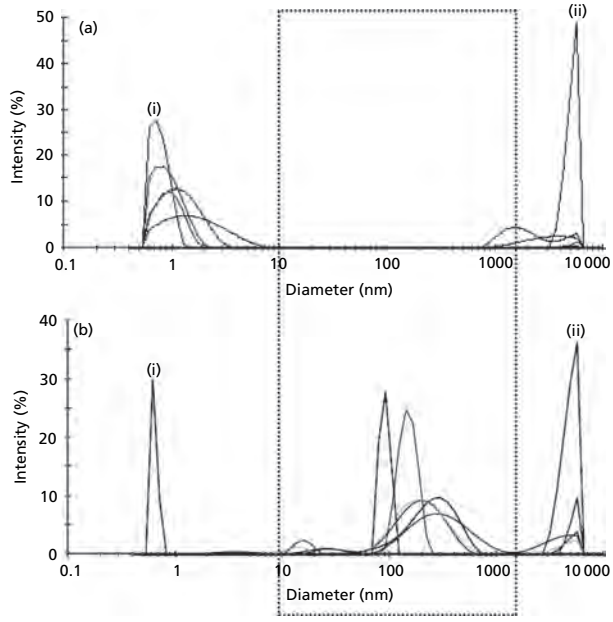

Figure 3 Intensity distributions by size, representing the aggregation pattern at different time intervals in polar and non-polar solvents. (a) Methanol (count rate 238 kcps). (b) Chloroform (count rate 3071 kcps). Peak (i) indicates the 0-min reading and peak (ii) indicates aggregation dynamics after 10 h. All other curves are in-between time points from 0 to 10 h. The dotted rectangle is representative of faster aggregation dynamics in chloroform. Results are a sum of accepted data collected.

(x – 25%) reduce the nucleation rate, leading to prolonged and gradual crystal growth, thus generating broader large-size laths (Figure 1h, i, j) (Ulrich & Strege 2002).

Effect of stirring

Stirring can have a profound effect on the crystallization product, particularly the crystal size distribution. The time that crystallization solutions were stirred (T_s) was selected based on the solvent's boiling point and time taken for complete evaporation of the solvent at a particular crystallization temperature.

In both polar and non-polar solvents, crystal size decreased with stirring, especially when stirring was done until time T_s. In polar solvents, small acicular crystals were observed irrespective of saturation and temperature. In non-polar solvents, however, the crystals obtained were broader under conditions where stirring was not performed until complete crystallization had occurred compared with solutions that had been stirred until complete crystallization occurred. The width of the crystals in these solvents increased with an increase in temperature from 5 to 60°C. Stirring increases both primary and secondary nucleation and promotes mass and heat transfer that enhances interfacial supersaturation and nucleation, resulting in the formation of relatively small crystals. It has been reported that increased frequency of collision overcomes the energy barrier desired for nuclei formation during primary nucleation whereas broken nuclei provide new sites for the crystal growth through secondary nucleation (Chow & Grant 1988). Reduction in crystal size is primarily contributed to by secondary nucleation, wherein nuclei result from intercrystal collisions, collisions between the stirrer bead and crystals, and between crystals and the walls of the container (Akal et al 1986). This imbalance between decreased crystal growth and increased nucleation rates led to small size crystals.

Crystallization using vapour diffusion

Table 2 gives the results of the vapour diffusion experiment. This technique involves equilibration between solvent and antisolvent vapours, followed by diffusion of antisolvent vapours into the drug solution, thus initiating crystallization (Mersmann 1999). Crystals could be observed after a relatively long lag time of 48–50 h, in contrast to 2–8 h required in the solvent recrystallization method. High local supersaturation in solvent recrystallization is reported to lead to fast aggregation of crystals as compared with vapour diffusion (Guillory 1999; Mersmann 1999), thus leading to clumping and poor quality of crystals. In contrast, the slow molecular aggregation in vapour diffusion allows the development of a well-defined three-dimensional array, with lower crystal defects (Garside 1985).

The lath-shaped crystals obtained from vapour diffusion (Figure 1k–l), defined as long thin blade-like crystals by USP (USP Convention 2000), were compared with the acicular crystals obtained using solvent recrystallization. The AR for needles and laths were over the range of 6–9 and 7–9, respectively. The range of AR for both isomorphs overlaps as an increase in breadth was also accompanied by an increase in length of the laths. However, a comparison based on width of the crystals revealed interesting findings (Table 2).

As observed from the photomicrographs (Figure 1k–o), even with vapour diffusion crystal broadening was observed, as the difference in the dielectric constant increased from 2.92 (in chloroform–hexane system) to 30.72 (in methanol–hexane system). However, tetrahydrofuran departed from the normal trend and exhibited needle-shaped morphology despite the small difference in dielectric constant (5.70 and 2.92 for tetrahydrofuran and chloroform, respectively) and similar boiling point (66°C) to chloroform (61°C). Also, a significant difference was observed in the width of crystals generated using tetrahydrofuran in comparison with other non-polar solvents. The tetrahydrofuran–hexane system generated crystals with a width of about 3 μm in contrast to the broad laths with a width of 41 μm in the chloroform–hexane system. This might be owing to the exceptionally high solubility of CEL in tetrahydrofuran (832 mg mL^{-1}) compared with other solvents such as chloroform, isopropanol and ethyl acetate (11, 11 and 137 mg mL^{-1}, respectively).

Characterization of crystallization products

The physicochemical characteristics of generated crystals were obtained using PXRD, DSC, TGA, HSM and FTIR. The purpose of these studies was to evaluate any possible polymorphic modification of CEL. Crystals obtained through solvent recrystallization under variable crystallization conditions and through vapour diffusion were found to be isomorphs of native acicular CEL (Chawla et al 2003). All characterization studies confirmed modification only in the crystal habit of

Table 2 Vapour diffusion experiments with different antisolvent and solvent combinations, with the results in terms of the obtained crystal habit and width of crystals

Antisolvent (bp°C)	Solvent (bp°C)	Polarity difference between solvent and antisolvent (based on dielectric constant)	Crystal habit	Width of crystals (μm)[a]
Hexane (68)	Chloroform (61.2)	2.92	Laths	41.34 ± 3.18
	Ethyl acetate (77.1)	4.14	Laths	34.98 ± 3.18
	Tetrahydrofuran (66)	5.70	Needles	3.18 ± 1.59
	Isopropanol (82.3)	18.08	Laths	34.98 ± 3.18
	Acetone (56.3)	18.82	Thin laths	15.90 ± 3.18
	Ethanol (78.3)	22.67	Thin laths	15.90 ± 3.18
	Methanol (64.7)	30.72	Thin laths	12.72 ± 3.18
Carbon tetrachloride (76.8)	Chloroform (61.2)	2.60	Laths	41.34 ± 3.18
	Ethyl acetate (77.1)	3.82	Laths	38.16 ± 3.18
	Tetrahydrofuran (66)	5.38	Needles	3.18 ± 1.59
	Isopropanol (82.3)	15.70	Laths	34.98 ± 3.18
	Acetone (56.3)	18.50	Thin laths	15.90 ± 3.18
	Ethanol (78.3)	22.35	Thin laths	12.72 ± 3.18
	Methanol (64.7)	30.40	Thin laths	12.72 ± 3.18
	Acetonitrile (81.6)	35.30	Needles	3.18 ± 1.59
Cyclohexane (80.7)	Chloroform (61.2)	2.80	Laths	38.16 ± 3.18
	Ethyl acetate (77.1)	4.02	Laths	34.98 ± 3.18
	tetrahydrofuran (66)	5.58	Needles	3.18 ± 1.59
	Acetone (56.3)	18.70	Thin laths	12.72 ± 3.18
	Ethanol (78.3)	22.50	Thin laths	12.72 ± 3.18

[a]For all solvents, the width of 50 particles was measured. A statistically significant difference was observed between laths, needles and thin laths on applying Kruskal–Wallis one-way analysis of variance on ranks ($P < 0.001$).

crystals and no polymorph and solvate formation. The recrystallized samples showed a single endothermic peak in DSC over the temperature range of 160.8–164.6°C (onset and endset) and identical values of heat of fusion (a measure of crystal lattice energy). In the TGA analysis, no weight loss was observed, indicating absence of solvate formation. This was also confirmed by HSM, as no evolution of bubbles was observed when samples were heated after mounting in oil. PXRD patterns of the recrystallized product depicted peaks, characteristic of pure CEL at 5.37°, 10.72°, 16.11°, 19.72°, and 21.52° 2θ values, although changes were observed in the intensity of the peaks probably due to variability in particle properties leading to different preferred orientations (Sarra et al 2002). The FTIR spectra were identical to acicular CEL with all main absorption bands. This confirmed that there was no difference between internal structure and conformation of laths and acicular crystals, and PXRD changes were not associated with any change at the molecular level.

AFM studies

AFM is an important tool for imaging the topography of samples, which is known to substantially affect the bulk properties of a material (Assender et al 2002). In the present study, tapping-mode AFM was used for surface topographical profiling since in the contact mode, the tip might damage the surface of samples (Trojak et al 2001).

Surface topographical features

Figure 4a shows the 2D AFM images for the laths and needles. A qualitative indication of the differences in roughness of two samples was obtained from the gray-scale index that depicts the height profile of the surface features. The surface of needles was found to be rougher compared with laths, which is even more clearly visible in the 3D AFM images (Figure 4b). The needles exhibited humps, undulations and features with greater heights (max. height of 28.75 nm) in comparison with laths where the maximum feature height was about 16.75 nm. A quantitative indication of the surface roughness (Figure 4b), in terms of root mean square roughness for the scan area of 2 μm × 2 μm, gave values of 2.92 and 1.79 nm for needles and laths, respectively. The highly undulated surface of needles would increase the surface area and the surface energy. The surface area of needles and laths was found to be 1.366 and 1.109 $m^2 g^{-1}$, respectively. This greater surface area of needles can hinder "slipping" of crystals over one another, thus affecting the flow and mixing properties of active pharmaceutical ingredients.

Flow properties

Powder flow can be affected by particle size, size distribution, shape, surface texture, surface energy, chemical composition, moisture content and other properties (Busignies et al 2004; Li et al 2004). The Hausner ratio and Carr's index of acicular crystals and laths, after sieving and addition of

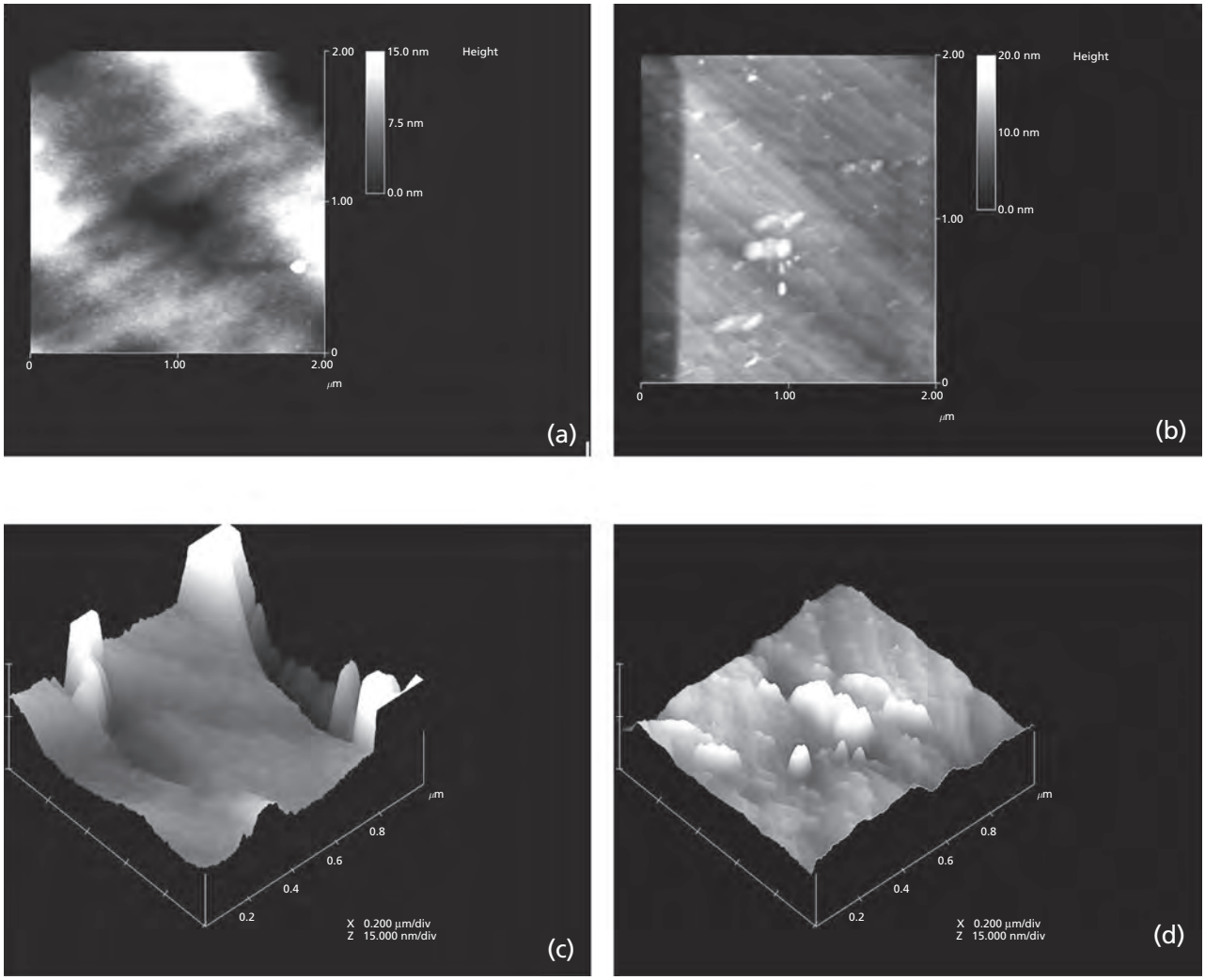

Figure 4 Atomic force microscopy (AFM) image of crystals at a scan rate of 1.507 Hz, scan size 2 μm, number of samples 256, and data scale 15.00 nm: (a) 2 μm × 2 μm surface topographical AFM image of needle surface; (b) 2 μm × 2 μm surface topographical AFM image of lath surface in tapping mode (light areas are indicative of high roughness while dark areas indicate smooth surface); (c) 3D profile for the 1 μm × 1 μm section of needle surface; (d) 3D profile for the 1 μm × 1 μm section of the needle surface.

Aerosil-200, are given in Table 3. Untreated lath samples exhibited poor flow behaviour compared with solvent recrystallization needles as evidences by the higher Carr's index value. The addition of 2% Aerosil-200 did not show any alteration in this trend. However, enhanced flow was observed when laths were passed through the BSS #18 sieve, which further improved on addition of 2% w/w Aerosil 200. The needles, on the other hand, did not show much improvement even after the addition of Aerosil-200 with sieving.

Compression studies

Crystal shape is a complex characteristic and its relation to powder properties is difficult to assess. Limited studies specifically discuss the relationship between shape and compaction behaviour (Tiwary & Panpali 1999). The contact area between particles in the die can vary depending on the alignment of particles, which can be affected even by exclusive

Table 3 Flow properties of needles and laths after different treatments

No.	Treatment	Habit	Carr's index	Hausner ratio
1[a]	–	Needle	38 ± 1.18	1.61 ± 0.08
		Laths	42 ± 0.98	1.72 ± 0.015
2[b]	2 % Aerosil 200	Needle	32 ± 1.34	1.47 ± 0.02
		Laths	40 ± 1.12	1.5 ± 0.012
3[c]	Sieving BSS #18	Needle	30 ± 0.76	1.42 ± 0.03
		Laths	20 ± 1.34	1.26 ± 0.01
4[d]	Sieving BSS #18	Needle	30 ± 0.80	1.42 ± 0.04
	+2 % Aerosil 200	Laths	16 ± 1.50	1.20 ± 0.01

Values are mean ± s.d., n = 3. [a]Differences in the mean values among groups were not great enough to exclude the possibility of random sampling variability; there was not a statistically significant difference. [b,c,d]A statistically significant difference between needles and laths was observed ($P < 0.001$).

variation of just the external structure (Rasenack & Muller 2002b).

Compression cycles or force–displacement curves can be divided into three steps: the first (up-curve) corresponds to rearrangement and packing of powder in the die, the second corresponds to fragmentation and/or plastic deformation of the particles, and during the third phase (down curve) the compact is instantaneously recovered elastically (Jetzer et al 1983). The area under the force–displacement curves obtained with the texture analyser was calculated for both isomorphs, which corresponded to the compression work (net work done). The values of net work done suggest that both the samples showed plastic deformation (with or without fragmentation). Net work done is the energy used in plastic deformation and bond formation. In contrast, for elastic materials, the work needed to deform is completely recovered during decompression and no work is used for compact formation (Jetzer et al 1983). Modified crystal habit (laths) showed lower Net work done (182.58 Nmm) than needles (275.34 Nmm), thereby confirming an improvement in compression behaviour. Due to their rough and high surface area (as evident from AFM studies) needles were observed to stick to the punches in contrast to laths. The rearrangement step was lower for laths and they showed a greater propensity to consolidate, probably due to the fact that there is a minor change in volume during packing. Elastic recovery was greater for laths (214.34 Nmm) than for needles (287.22 Nmm), resulting from lower interparticulate bonding.

Crystal habit affects the initial particle rearrangement, which in turn affects the compaction profile. The triclinic class of crystals, as in celecoxib, possess low symmetry and the relative orientation of crystallites during compression influences the mechanical properties of the compact. Orientation of crystal faces during compression may significantly affect the overall mechanical properties of the compact (Bandopadhyay & Grant 2002). More equidimensional crystals such as sieved laths in this case (AR 2–4) orient randomly and demonstrate less anisotropy during compression in contrast to needles. Estimation of the crystal morphology by the Bravais-Friedel Donnay Harker model predicted {0 1 0} to be the slowest growing and most dominant facet occupying 50.43% of the area (data not shown). Thus, it is expected that this face would govern the physiochemical properties of the crystal. This would have implications both in tableting and in capsules manufactured using the tamping capsule filling mechanism. The latter involves formation of a loose slug of powder, followed by transfer to the capsule shell. However, further compression studies need to be done to explain the deformation behaviour of CEL and its isomorphs.

Conclusion

Drug substances crystallizing as needles show poor mechanical properties, but their shape can be modified by crystal engineering. The concept that different crystal modifications arise under varied experimental conditions demands the use of diverse crystallization approaches to reveal the spectrum of polymorphs and isomorphs. Reproducibility can be ensured by defining the occurrence domain (which describes the experimental conditions in which a substance crystallizes into a particular solid form), but requires meticulous consideration of external crystallization parameters. CEL crystallized using conventional solvent recrystallization approach forms cohesive and agglomerating needles, having low bulk density and poor processability. However, modified habit (AR 2–4) with better handling properties could be generated by altering the balance between crystal growth and nucleation through parameters such as solvent polarity, solute concentration, temperature and stirring. The generated isomorphs can further be used as seeds to produce the desired habit with improved processability on a larger scale. Therefore, fundamental aspects of crystallization kinetics can be exploited to commercially produce crystals with improved processability.

References

Akal, M.M., Zakaria, M., Ebrahim, A., Nassar, M.M. (1986) Secondary nucleation rate of sodium chloride under different stirring conditions. *J. Cryst. Growth* **78**: 528–532

Assender, H., Bliznyuk, V., Porfyrakis, K. (2002) How surface topography relates to materials' properties. *Science* **297**: 973–976

Bandyopadhyay, R. Grant, D. W. J. (2002) Plasticity and slip system of plate-shaped crystals of l-lysine monohydrochloride dehydrate. *Pharm. Res*. **19**: 491–496

Berkovitch-Yellin, Z. (1985) Toward an ab initio derivation of crystal morphology. *J. Am. Chem. Soc*. **107**: 8239–8253

Brittain, H.G. (2001) Particle size distribution, part 1, representations of particle shape, size, and distribution. *Pharm. Tech*. **25**: 38–45

Busignies, V., Tchoreloff, P., Leclerc, B., Besnard, M., Couarraze, G., (2004) Compaction of crystallographic forms of pharmaceutical granular lactose. I. Compressibility. *Eur. J. Pharm. Biopharm*. **58**: 569–576

Cang, H. X., Bi, R.C. (1998) Nuclear studies on the pre-nucleation transport in the liquid/liquid diffusion crystallization of proteins. *J. Cryst. Growth* **194**: 133–137

Chawla, G., Gupta, P., Thilagavathi, R., Chakraborti, A. K., Bansal, A. K. (2003) Characterization of solid-state forms of celecoxib. *Eur. J. Pharm. Sci*. **20**: 305–317

Chow, A. H. L., Grant, D. J. W. (1988) Modification of acetaminophen crystals. II. Influence of stirring rate during solution-phase growth on crystal properties in the presence and absence of p-acetoxyacetanilide. *Int. J. Pharm*. **41**: 29–39

FDA (1987) Guideline for submitting supporting documentation in drug applications for the manufacture of drug substance. Available from: http://www.fda.gov/cder/guidance

Ferro, L.J., Miyake, P. J. (2001) Polymorphic crystalline forms of celecoxib. WO 01/42222 A1

Ferro, L.J., Miyake, P. J. (2004) Polymorphic crystalline forms of celecoxib. US 0087640A1

Garside, J. (1985) Industrial crystallization from solution. *Chem. Eng. Sci*. **40**: 3–26

Goddard, L.E. (1998) Process for improving flow characteristics of crystalline ibuprofen. US patent 5843863

Granberg, A., Bloch, D.G., Rasmuson, A. C. (1999) Crystallization of paracetamol in acetone-water mixtures. *J. Cryst. Growth* **199**: 1287–1293

Grant, D. J. W. (1999) Theory and origin of polymorphism. In: Brittain, H. G. (ed.) *Polymorphism in pharmaceutical solids*. Marcel Dekker, New York, pp 1–33

Gua, C. H, Lib, H., Gandhi, R. B., Raghavana, K. (2004) Grouping solvents by statistical analysis of solvent property parameters: implication to polymorph screening. *Int. J. Pharm*. **283**: 117–125

Guillory, J. K. (1999) Generation of polymorphs, hydrates, solvates and amorphous solids. In: Brittain, H. G. (ed.) *Polymorphism in pharmaceutical solids*. Marcel Dekker, New York, pp 227–278

Hornedo, N. R., Murphy, D. (1999) Significance of controlling crystallization mechanisms and kinetics in pharmaceutical systems. *J. Pharm. Sci*. **88**: 651–660

Hulliger, J. (1994) Chemistry and crystal growth. *Angew. Chem. Int. Ed. Engl*. **33**: 143–162

ICH Harmonized Tripartite Guideline (1997) Impurities: Guidelines for Residual Solvents. ICH Q3C

Jetzer, W., Leuenberger, H., Sucker, H. (1983) The compressibility and compactibility of pharmaceutical powders. *Pharm. Tech*. **4**: 33–39

Lahva, M., Leiserowitz, M. (2001) The effect of solvent on crystal growth and morphology. *Chem. Eng. Sci*. **56**: 2245–2253

Li, Q., Rudolph, V., Weigl, B., Earl, A. (2004) Interparticle van der Waal force in powder flowability and compactibility. *Int. J. Pharm*. **280**: 77–93

Martin, A., Bustamante, P., Chun, A. H. C. (1997) Micromeritics. In: Martin, A., Bustamante, P., Chun, A. H. C. (eds) *Physical pharmacy*. B. I. Waverly Pvt. Ltd, New Delhi, pp 423–452

Mersmann, A. (1999) Crystallization and precipitation. *Chem. Eng. Process*. **38**: 345–353

Nokhodchi, A., Bolourtchian, A., Dinarvand, R. (2003) Crystal modification of phenytoin using different solvents and crystallization conditions. *Int. J. Pharm*. **250**: 85–97

Rasenack, N., Muller, B. W. (2002a) Properties of Ibuprofen crystallized under various conditions: a comparative study. *Drug Dev. Ind. Pharm*. **28**: 1077–1089

Rasenack, N., Muller, B. W. (2002b) Crystal habit and tableting behavior. *Int. J. Pharm*. **244**: 45–57

Sarra, N., Roberts, C., Williams, A. C., Grimsey, I. M., Booth, S. W. (2002) Quantitative analysis of mannitol polymorphs. X-ray powder diffractometry-exploring preferred orientation effects. *J. Pharm. Biomed. Anal*. **28**: 1149–1159

Shekunov, Y. B., York, P. (2000) Crystallization processes in pharmaceutical technology and drug delivery design. *J. Cryst. Growth* **211**: 122–136

Takubo, H., Kume, S. (1984) Relationships between supersaturation, solution velocity, crystal habit, and growth rate in crystallization of $NH_4H_2PO_4$. *J. Cryst. Growth* **67**: 217–226

Tiwary, A. K. (2001) Modification of crystal habit and its role in dosage form performance. *Drug Dev. Ind. Pharm*. **27**: 699–709

Tiwary, A. K., Panpali, G. M. (1999) Influence of crystal habit on trimethoprim suspension formulation. *Pharm. Res*. **16**: 261–265

Trojak, A., Kocjevar, K., Musjevicj, L., Srcjicj, S. (2001) Investigation of the felodipine glassy state by atomic force microscopy. *Int. J. Pharm*. **218**: 145–151

Ulrich, J., Strege, C. (2002) Some aspects of the importance of metastable zone width and nucleation in industrial crystallizers. *J. Cryst. Growth* **237**–**239**: 2130–2135

USP Convention (2000) Optical Microscopy, General Tests (776). USP, Rockville, MD